Pergamon

Ultrasound in Med. & Biol., Vol. 21, No. 3, pp. 379–391, 1995

0301-5629/95 $9.50 + .00

0301-5629(94)00126-X

●*Original Contribution*

IN SITU HUMAN OBSTETRICAL ULTRASOUND EXPOSIMETRY: ESTIMATES OF DERATING FACTORS FOR EACH OF THREE DIFFERENT TISSUE MODELS

TARIQ A. SIDDIQI,[†] WILLIAM D. O'BRIEN, JR.,[‡] RICHARD A. MEYER,[*] JOAN M. SULLIVAN[†] and MENACHEM MIODOVNIK[†]

[†]Department of Obstetrics and Gynecology, University of Cincinnati Medical Center, 231 Bethesda Avenue, Cincinnati, OH 45267; [‡]Department of Electrical and Computer Engineering, University of Illinois, 1406 West Green Street, Urbana, IL 61801; and [*]Division of Cardiology, Children's Hospital Medical Center, Elland and Bethesda Avenues, Cincinnati, OH 45229, USA

(*Received* 21 *February* 1994; *in final form* 11 *August* 1994)

Abstract—A specialized *in vivo* exposimetry system was developed to acquire transabdominal *in situ* ultrasound exposure quantities in obstetric patients. Under surgical conditions, the sterilized 7-element calibrated linear array hydrophone was introduced into the uterus under direct ultrasound guidance and placed in direct contact with the products of conception, usually in the saggital midplane of the uterine cavity. Twenty-five patients with empty bladders and 10 patients with full bladders were studied at gestational ages between 7 and 20 weeks. In the empty bladder condition, the sound beam traversed the anterior abdominal wall, uterus, amniotic fluid and fetal parts and in the full bladder condition, the sound beam also traversed the fluid-filled bladder. Each study was conducted with a 3 MHz, mechanical sector transducer in combination with an ATL Ultramark 4 diagnostic ultrasound imaging system. Calibration data were recorded after completion of each *in vivo* patient study. The acquired exposimetry data from the 35 obstetric patients were used to evaluate the appropriateness of three tissue attenuation models, *viz., fixed path, homogeneous* and *overlying*. All three tissue models yield a mean attenuation coefficient value of about a factor of 3 to 4 greater than their respective minimum values. In the case of the *overlying* and *homogeneous* tissue models, there was a statistically significant correlation between their calculated attenuation coefficients and total distance for the combined data set whereas there was no such dependency for the calculated *fixed-path* tissue model. In summary, any one of the three tissue models may be used to estimate *in utero* acoustic quantities during the first and second trimesters of human pregnancy based on this study.

Key Words: **Ultrasound, Bioeffects, Exposimetry, Dosimetry, Tissue modeling, Derating factor, *In situ* exposimetry, *In vivo* exposimetry, *In utero* exposimetry, Obstetrics.**

INTRODUCTION

Ultrasonic dosimetry (O'Brien 1992) is concerned with the quantitative determination of ultrasonic energy interaction with biological materials, that is, defining the quantitative relationship between an ultrasound exposure level and the biological effect it produces. Embryo and fetal ultrasound bioeffects have been extensively reviewed over the past few years (AIUM 1988, 1993; Miller and Ziskin 1989; NCRP 1983, 1992; NIH 1984; Taran-tal and O'Brien 1994; O'Brien 1991; WFUMB 1989, 1992; Ziskin and Pittiti 1988). Overall, some conclusions can be drawn from these reports. If ultrasound as a physical agent were capable of inducing gross malformations, then a rise in the occurrence of birth defects would have been documented by now, although a very small rise may not be detectable without extremely large sample sizes. This has not been the case, as epidemiological studies have shown no significant correlations between a rise in its use and the incidence of congenital anomalies. However, based on the fact that results of experimental studies have proven inconsistent, it is clear that the interaction of ultrasound with biological systems, particularly those with rapidly dividing cells, is still not fully understood. What remains of concern are the subtle and/or long-term manifestations of frequent intrauterine exposure. These concerns remain pertinent due to a number of factors such as the continued rise in the percentage of the prenatal population that is ex-

Address correspondence to: Tariq A. Siddiqi, M.D.

posed each year. In addition, as advances in technology are made, the exposure parameters for the fetus can also change. The use of pulsed Doppler (and color flow imaging) are good examples; these methods have been applied more recently for evaluating physiologic function and rely on time-average output parameters that are greater than those for routine imaging. The exposure time may also be increased as additional diagnostic information is sought. These points emphasize the need to pursue these questions in an effort to confirm that unwanted effects do not occur.

The recently approved Output Display Standard (AIUM/NEMA 1992) addresses one aspect of ultrasound dosimetry in which the user of diagnostic ultrasound equipment is provided with quantitative indices which relate to temperature increase, the thermal index, and the potential for cavitation, the mechanical index, from the diagnostic ultrasound field. In its development, certain aspects of the tissue in which the ultrasound wave propagated had to be assumed in order to estimate *in situ* ultrasound exposure levels. Ultrasound exposimetry, a necessary component of ultrasound dosimetry, is thus concerned with the quantitative determination of ultrasonic exposure levels in biological materials and the development of quantitative tissue models is a necessary part of such studies.

There is, therefore, a need for realistic tissue models to predict *in situ* acoustic exposure levels from measurements of acoustic output made in water in order to have an improved basis for estimating risk. Both national (AIUM 1988, 1993; AIUM/NEMA 1992; NCRP 1983, 1992) and international (WFUMB 1989, 1992) organizations, as well as research groups (Akaiwa 1989; Carson et al. 1989; Carson 1989; Ramnarine et al. 1993; Siddiqi et al. 1991, 1992; Smith et al. 1985), have been evaluating and/or developing models and guidelines. For example, the US Food and Drug Administration (FDA 1985, 1993) uses a homogeneous tissue model, also referred to as a derating model, in their 510(k) process which is required by manufacturers and importers of diagnostic ultrasound devices in the United States to estimate *in situ* exposure levels. The homogeneous tissue model assumes that the propagated ultrasound wave travels through a uniform tissue medium with a derating factor of 0.3 dB/cm-MHz. It could be argued that this derating factor is conservative, that is, its application will generally yield an *in situ* acoustic exposure level greater than the actual *in situ* level because the tissue attenuation is greater than 0.3 dB/cm-MHz. However, for fetal imaging applications where the propagated ultrasound wave traverses through the fluid-filled bladder fluid, it could be argued that this derating factor is reasonable when the tissue path consists of 60% soft tissue (attenuation assumed to be 0.5 dB/cm-MHz) and 40% fluid (attenuation assumed to be negligible). If the total traversed path consists of more than 40% fluid, then it could be argued that this derating factor underestimated the *in situ* acoustic exposure levels.

In human pregnancy, the embryonic stage of development includes the first eight weeks after fertilization. This is the period of cell division and organogenesis which is complete once the human embryo enters the fetal stage. Any damage to dividing cells or organelles at this stage may translate into major abnormalities at birth. Experimental data provide almost no information with respect to the threshold levels of ultrasound for the induction of lethal and nonlethal abnormalities and where existing, such data are conflicting. As an essential first step, it is critical to determine the actual ultrasonic levels to which the human embryo is exposed. We have constructed a specialized *in vivo* exposimetry system, developed and tested customized software and determined selected first-order and second-order ultrasonic field quantities during a routine reproductive ultrasound examination of the human ovary (Daft et al. 1990; Siddiqi et al. 1991).

Using the previously described customized equipment, the current study was designed to determine selected first-order and second-order ultrasonic field quantities to which the human embryo and fetus are exposed during the course of a "routine" diagnostic ultrasound examination. As a first step towards determining risk, we used these experimentally obtained exposure data to estimate the appropriate derating factor for each of three proposed clinical tissue models for ultrasound dosimetry calculations in the obstetric patient: (1) *Fixed path* (fp), (2) *Homogeneous* (ho), (3) *Overlying* (ov).

METHODS

Diagnostic imaging system

A 3.0 MHz frequency, mechanical sector transducer (depth of focus 5.5–13 cm, focal length 8 cm, crystal diameter 19 mm) in combination with an ATL Ultramark 4 Model (Advanced Technology Laboratories, Bothel, WA, USA) diagnostic ultrasound imaging system was used for all studies. Exposure time after obtaining an acceptable real-time image was 5 min. Power setting for the system was 100% at all times.

Exposimetry instrumentation

The customized exposimetry equipment and software for *in vivo* and calibration (*in vitro*) measurements have been previously reported in detail (Siddiqi et al. 1991). In summary, instrumentation has been

developed to measure acoustic pressure (AIUM/NEMA 1992) during a diagnostic reproductive system ultrasound examination. The acoustic pressure field is sampled using a calibrated 7-element linear array hydrophone of polyvinylidine difluoride transducers, which is introduced into the uterus through the dilated cervix in a sterile fashion, and placed in contact with the nonviable human embryo using real-time imaging. The radio-frequency (RF) signals from the hydrophone are digitized at 50 megasamples per second and the received temporal waveform which has the maximum amplitude in the examination is recorded. The reference output of the clinical real-time scanner is obtained by placing the hydrophone in a temperature controlled (37°C) water bath at the same range from the clinical transducer as that used to obtain the *in vivo* temporal waveform recording. From the digitized hydrophone recordings, 10 exposimetry quantities are estimated, 5 under *in vivo* conditions and 5 in the water tank, that is, *in vitro* conditions. The 5 quantities for each condition are the peak compressional pressure, p_c, the peak rarefactional pressure, p_r, the temporal peak intensity, I_{TP}, the pulse average intensity, I_{PA}, and the temporal average intensity, I_{TA} (AIUM 1992; Daft et al. 1990; Siddiqi et al. 1991, 1992).

Patient population

Otherwise healthy first- and second-trimester pregnant subjects with a sonographically confirmed diagnosis of missed abortion were recruited to the study after the clinical decision to perform a dilatation and curettage had been made by their primary physician. Each subject was counseled and asked to sign an informed consent statement as approved by the University of Cincinnati Medical Center Institutional Review Board. Each subject was studied only once for data analysis.

The patients were divided into two groups: Group EB (25 subjects: 15 first trimester and 10 second trimester) was comprised of subjects whose bladder was empty and the ultrasound beam traversed the anterior abdominal wall, uterine wall and amniotic fluid prior to visualization of the hydrophone which was in contact with the products of conception in the uterine cavity (Fig. 1); Group FB (10 subjects: 9 first trimester and 1 second trimester) was comprised of subjects who had a full bladder and the ultrasound beam traversed the anterior abdominal wall, distended bladder, uterine wall and amniotic fluid prior to visualization of the hydrophone which was in contact with the products of conception in the uterine cavity (Fig. 2). Overall patient size and the presence or absence of a distended urinary bladder therefore affected the total distance between the abdominal wall skin surface (transducer) and the products of conception (hydrophone).

Hydrophone placement and study protocol

For first-trimester patients, each patient was prepped and draped in the usual fashion for a first-trimester dilatation and curettage. After appropriate anesthesia had been administered by either the responsible anesthesiologist or primary care physician, a self-retaining vaginal speculum was inserted and the cervix was visualized and cleansed together with the vagina with an antiseptic solution (betadine). The cervix was then dilated with graduated dilators in a standard fashion. At this time, one of the authors (TAS) who was also scrubbed for surgery introduced the sterilized exposimetry hydrophone into the uterus under direct ultrasound guidance. The hydrophone was placed in direct contact with the products of conception, usually in the saggital midplane of the uterine cavity. The lower end of the hydrophone has a recognizable round flange to help ensure appropriate placement and orientation of the linear array of transducers. The thicknesses of each of the previously listed tissue layers between the transducer and the hydrophone were then measured separately as well as the total distance between the transducer and the hydrophone.

In a similar fashion, second-trimester patients undergoing prostaglandin induction of abortion, were studied by inserting the exposimetry hydrophone into the uterine cavity using sterile technique prior to administration of prostaglandin E_2 20 mg suppositories.

In vivo data were then obtained at 100% power setting of the diagnostic imaging system. In summary, the transducer was moved across the abdominal wall surface with real-time imaging ensuring constant hydrophone visualization. The largest hydrophone signal was saved for analysis. Reference (*in vitro*) data were recorded immediately after completion of each of the *in vivo* studies from a tank filled with water at body temperature (37°C) and with the transducer and hydrophone fixed at the same total distance as the *in vivo* state. Again, the largest signal recorded during the *in vitro* procedure was saved for data analysis.

Data analysis

For each subject, one complete data set of *in vivo* and *in vitro* acoustic pressure waveforms was obtained with a corresponding sonogram for total distance and tissue thickness measurements. Six acoustic insertion loss (*IL*) values (loss as determined by the measurement procedure) were calculated for each subject, *i.e.*,

$$IL = -20 \log_{10}\left(\frac{\textit{in vivo}\ \text{pressure}}{\textit{in vitro}\ \text{pressure}}\right) \text{(in dB)} \quad (1)$$

Fig. 1. Sonogram of EB example showing anterior abdominal wall, uterine wall, fetal head (curved arrow) and hydrophone (straight arrow).

where the pressure ratios were for p_c, p_r and $p_c + p_r$, and

$$IL = -10 \log_{10}\left(\frac{\textit{in vivo} \text{ intensity}}{\textit{in vitro} \text{ intensity}}\right) \text{(in dB)} \quad (2)$$

where the minus sign was used to represent the IL values as positive numbers for subsequent analyses and where the intensity ratios were for I_{TA}, I_{PA} and I_{TP}. For subsequent calculations, a mean insertion loss value was determined from

Fig. 2. Sonogram of FB example showing anterior abdominal wall, distended bladder (white arrow), uterine wall, amniotic fluid and hydrophone (black arrow).

Table 1. Mean value ± standard deviation (range) of measured and calculated quantities for the first-trimester versus second-trimester comparison (empty bladder group).

	First trimester (n = 15)	Second trimester (n = 10)	1st versus 2nd trimester p value†	Trimesters combined (n = 25)
$\langle GA \rangle_g$ (weeks)	9.4 ± 1.6 (7–12)	17 ± 2.1 (14–20)	0.0001	12 ± 4.1 (7–20)
$\langle d_{\text{abd wall}} \rangle_g$ (cm)	2.0 ± 0.74 (1.4–3.7)	2.5 ± 0.84 (1.2–4.0)	0.18	2.2 ± 0.80 (1.2–3.7)
$\langle d_{\text{uterus}} \rangle_g$ (cm)	2.4 ± 1.7 (0.4–5.3)	1.0 ± 0.38 (0.7–2.0)	0.0083‡	1.8 ± 1.5 (0.4–5.3)
$\langle d_{\text{am fluid}} \rangle_g$ (cm)	2.1 ± 1.5 (0–4.6)	0.85 ± 1.1 (0–3.0)	0.036	1.6 ± 1.4 (0–4.6)
$\langle d_{\text{fetal parts}} \rangle_g$ (cm)	—	4.0 ± 1.3 (1.6–5.2)		
$\langle d_{\text{ov}} \rangle_g$ (cm)	4.4 ± 2.2 (1.9–9.0)	7.5 ± 1.5 (4.9–9.9)	0.0008	5.6 ± 2.4 (1.9–9.9)
$\langle d_{\text{total}} \rangle_g$ (cm)	6.5 ± 1.4 (4.4–9.0)	8.3 ± 1.7 (5.6–12)	0.0065	7.2 ± 1.8 (4.4–12)
$\langle IL \rangle_g$ (dB)	8.5 ± 5.4 (2.7–20)	10.5 ± 6.0 (4.1–23)	0.41	9.3 ± 6.0 (2.7–23)
$\langle A_{\text{fp}} \rangle_g \left(\frac{\text{dB}}{\text{MHz}}\right)$	3.6 ± 2.2 (1.1–8.2)	4.4 ± 2.5 (1.7–9.6)	0.41	3.9 ± 2.3 (1.1–9.6)
$\langle A_{\text{ho}} \rangle_g \left(\frac{\text{dB}}{\text{cm MHz}}\right)$	0.57 ± 0.37 (0.21–1.4)	0.56 ± 0.35 (0.16–1.1)	0.98	0.56 ± 0.36 (0.16–1.4)
$\langle A_{\text{ov}} \rangle_g \left(\frac{\text{dB}}{\text{cm MHz}}\right)$	0.97 ± 0.62 (0.27–2.1)	0.60 ± 0.33 (0.19–1.1)	0.98‡	0.82 ± 0.55 (0.19–2.1)

† Student t test unless otherwise noted; ‡ Welch t test.

$$\langle IL \rangle = \frac{1}{6} \sum_{i=1}^{6} IL_i \text{ (in dB)} \qquad (3)$$

where IL_i represents the six individual IL values for the same subject. The subscript "g" represents data grouping, such as first vs. second trimester or empty vs. full bladder, *e.g.*,

$$\langle IL \rangle_g = \frac{1}{25} \sum_{i=1}^{25} \langle IL \rangle \text{ (in dB)} \qquad (4)$$

where $\langle IL \rangle_g$ is the mean value of the 25 patients in the empty bladder group.

The $\langle IL \rangle$ was determined as previously described (Daft et al. 1990; Siddiqi et al. 1991, 1992). The $\langle IL \rangle$ in dB for each subject represents:

$$\langle IL \rangle = IL_{\text{abd wall}} + IL_{\text{bladder}} + IL_{\text{uterus}} + IL_{\text{am fluid}} + IL_{\text{fetal parts}} \text{ (in dB)} \qquad (5)$$

where $IL_{\text{abd wall}}$, IL_{bladder}, IL_{uterus}, $IL_{\text{am fluid}}$ and $IL_{\text{fetal parts}}$ are the individual insertion loss values for the abdominal wall, bladder (IL_{bladder} assumed zero for EB group), uterus, amniotic fluid and fetal parts, respectively. These individual loss values were not measured separately. Only $\langle IL \rangle$ was calculated from the *in vivo* and *in vitro* acoustic pressure measurements (see eqn 3) using a customized exposimetry system (Daft et al. 1990). The total distance (d_{total}) between the skin surface and the hydrophone is the sum of the individual thicknesses, that is,

$$d_{\text{total}} = d_{\text{abd wall}} + d_{\text{bladder}} + d_{\text{uterus}} + d_{\text{am fluid}} + d_{\text{fetal parts}} \text{ (in cm)} \qquad (6)$$

where $d_{\text{abd wall}}$, d_{bladder}, d_{uterus}, $d_{\text{am fluid}}$ and $d_{\text{fetal parts}}$ are the individual thicknesses for the abdominal wall, bladder (d_{bladder} assumed zero for EB group), uterus, amniotic fluid and fetal parts, respectively. The individual distance (thickness) measurements were made on-line using electronic calipers.

Calculations were based on three published tissue models, *viz.*, fixed path (Carson et al. 1989; NCRP 1992; Siddiqi et al. 1991), homogeneous (FDA 1985, 1993; NCRP 1992) and overlying (Daft et al. 1990; Siddiqi et al. 1991, 1992). The power spectra of the *in vivo* and *in vitro* pressure waveforms exhibited a maximum at about 2.4 MHz and therefore, for these three tissue models, 2.4 MHz was used for the center frequency, f_c.

The "*fixed-path*" (fp) tissue model is based on the assumptions that the ultrasonic attenuation between

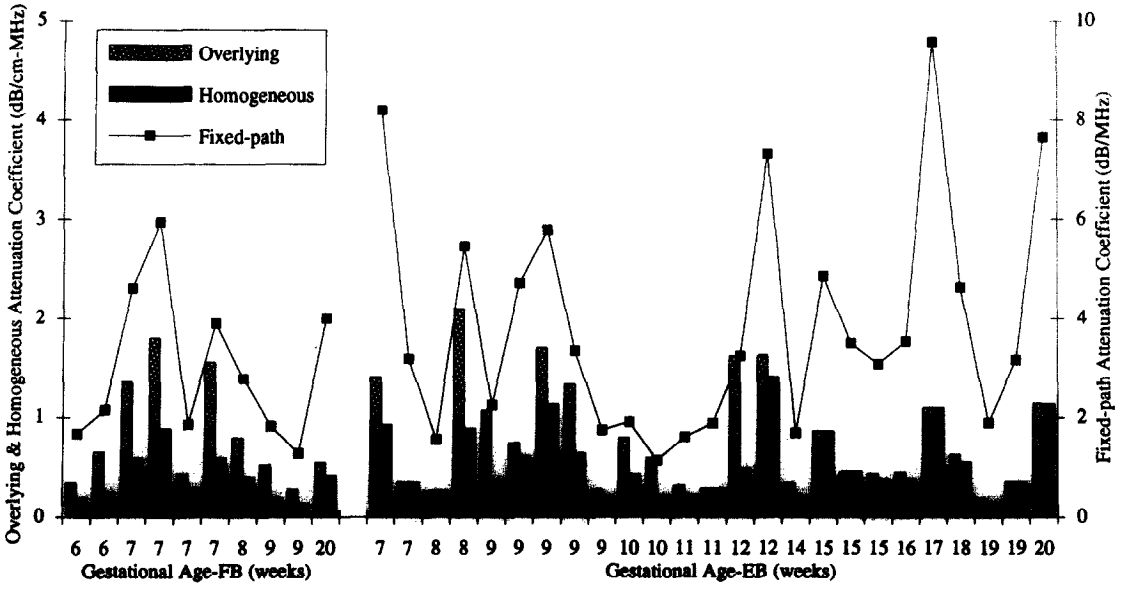

Fig. 3. Summary of the attenuation coefficients for the three tissue models for both the full bladder (FB) and empty bladder (EB) conditions as a function of gestational age.

the skin surface and conceptus is linearly dependent upon frequency and independent of distance (Carson et al. 1989; NCRP 1992; Siddiqi et al. 1991). The *fixed-path* attenuation coefficient for each subject is determined by the eqn

$$A_{\mathrm{fp}} = \frac{\langle IL \rangle}{f_c} \left(\text{in} \frac{\text{dB}}{\text{MHz}} \right) \tag{7}$$

where $\langle IL \rangle$ is the mean insertion loss in dB (see eqn 3) and f_c is the center frequency in MHz for each subject.

The "*homogeneous*" (ho) tissue model is based on the assumption that the ultrasonic attenuation occurs uniformly over the total distance between the skin surface and the conceptus (FDA 1985, 1993; NCRP 1992). The *homogeneous* attenuation coefficient for each subject is determined by the eqn

$$A_{\mathrm{ho}} = \frac{\langle IL \rangle}{d_{\mathrm{total}} f_c} \left(\text{in} \frac{\text{dB}}{\text{cm MHz}} \right). \tag{8}$$

The "*overlying*" (ov) tissue model is based on the assumptions that the ultrasonic attenuation occurs uniformly within intact tissue *only* and that there is negligible attenuation from any intervening fluid path (Daft et al. 1990; Siddiqi et al. 1991, 1992). The *overlying* attenuation coefficient for each subject is determined by the eqn

$$A_{\mathrm{ov}} = \frac{\langle IL \rangle}{d_{\mathrm{ov}} f_c} \left(\text{in} \frac{\text{dB}}{\text{cm MHz}} \right) \tag{9}$$

where d_{ov} is the thickness of the overlying intact tissue between the skin surface and conceptus and is determined by subtracting from the total distance all intervening fluid path distances, *i.e.*,

$$d_{\mathrm{ov}} = d_{\mathrm{total}} - d_{\mathrm{bladder}} - d_{\mathrm{am\ fluid}} \text{ (in cm)}. \tag{10}$$

Statistical methods

The two-tailed, unpaired Student t test was used to compare the means of the two unpaired groups with equivalent standard deviations. The assumption of equivalent standard deviations was tested with an F test. When the standard deviations were unequal, the two-tailed, unpaired Welch t test was used to compare the means of the two unpaired groups. Linear regression analysis was used to quantify the best-fit straight line between two variables. The slope's p value indicates the slope's significance relative to a zero slope and the adjusted sample coefficient of determination (adj r^2) accounts for the variation in the dependent variable. The adj r^2 is the sample coefficient of determination (r^2) adjusted for degrees of freedom (Hamburg 1979). The ±90% confidence intervals of the mean of the dependent variable are provided when the regression equation is shown graphically. Multiple regression analysis was used to quantify the best-fit estimate between more than two variables and the p

Table 2. Mean value ± standard deviation (range) of measured and calculated quantities for the empty bladder (EB) versus full bladder (FB) comparison.

	EB group (n = 25)	FB group (n = 10)	EB versus FB p value†	Groups combined (n = 35)
$\langle GA \rangle_g$ (Weeks)	12 ± 4.1 (7–20)	8.6 ± 4.1 (6–20)	0.02	11.3 ± 4.4
$\langle d_{\text{abd wall}} \rangle_g$ (cm)	2.2 ± 0.80 (1.2–4.0)	2.0 ± 0.54 (1.2–2.9)	0.38	2.2 ± 0.73
$\langle d_{\text{bladder}} \rangle_g$ (cm)	—	2.5 ± 1.1 (0.8–4.0)		
$\langle d_{\text{uterus}} \rangle_g$ (cm)	1.8 ± 1.5 (0.4–5.3)	2.1 ± 1.1 (0.8–4.4)	0.60	1.9 ± 1.4
$\langle d_{\text{am fluid}} \rangle_g$ (cm)	1.6 ± 1.4 (0–4.6)	1.4 ± 0.96 (0–3.3)	0.68	1.5 ± 1.3
$\langle d_{\text{fetal parts}} \rangle_g$ (cm)	4.0 ± 1.3* (1.6–5.2)	—		
$\langle d_{\text{ov}} \rangle_g$ (cm)	5.6 ± 2.4 (1.9–9.9)	4.1 ± 1.3 (2.5–7.3)	0.06	5.2 ± 2.3
$\langle d_{\text{total}} \rangle_g$ (cm)	7.2 ± 1.8 (4.4–12)	8.0 ± 1.2 (6.5–10)	0.022‡	7.4 ± 1.6
$\langle IL \rangle_g$ (dB)	9.3 ± 6.0 (2.7–23)	7.2 ± 3.7 (3.1–14)	0.28	8.7 ± 5.2
$\langle A_{\text{fp}} \rangle_g \left(\frac{\text{dB}}{\text{MHz}}\right)$	3.9 ± 2.3 (1.1–9.6)	3.0 ± 1.5 (1.3–5.9)	0.28	3.6 ± 2.2
$\langle A_{\text{ho}} \rangle_g \left(\frac{\text{dB}}{\text{cm MHz}}\right)$	0.56 ± 0.36 (0.16–1.4)	0.40 ± 0.23 (0.14–0.89)	0.18	0.52 ± 0.33
$\langle A_{\text{ov}} \rangle_g \left(\frac{\text{dB}}{\text{cm MHz}}\right)$	0.82 ± 0.55 (0.19–2.1)	0.83 ± 0.54 (0.28–1.8)	0.96	0.82 ± 0.54

† Student t test unless otherwise noted; ‡ Welch t test; * n = 10.

values are determined for each of the estimated coefficients to test their significant differences from zero. Statistical significance is assumed at the 0.05 level and all statistical calculations were performed using SAS Software (Cary, NC, USA).

RESULTS

First versus second trimester

The 25 patients studied in the empty bladder (EB) group consisted of 15 first-trimester and 10 second-trimester subjects (see Table 1). The two groups were statistically significantly different only in terms of selected physical dimensions, *viz.*, uterus distance (p = 0.0083), amniotic fluid distance (p = 0.036) and total distance (p = 0.0065) as well as overlying distance (p = 0.0008). However, there were no statistically significant differences in the calculated quantities of $\langle IL \rangle$, or the attenuation coefficients for the three tissue models (see Fig. 3). Figure 3 shows graphically that there are no obvious trends of the attenuation coefficients for the three tissue models as a function of GA. Therefore, the first- and second-trimester empty bladder results are combined for subsequent analyses.

Insertion loss

Group values (mean ± standard deviations and ranges) for all of the measured (intact tissue and fluid path distances) and calculated quantities ($\langle IL \rangle_g$, $\langle A_{\text{fp}} \rangle_g$, $\langle A_{\text{ho}} \rangle_g$ and $\langle A_{\text{ov}} \rangle_g$) for the two groups, full bladder (FB) and empty bladder (EB), are shown in Table 2. The $\langle IL \rangle_g$ values for the EB (n = 25) and FB (n = 10) groups were 9.3 ± 5.6 dB and 7.2 ± 3.7 dB, respectively, and were not statistically significantly different (p = 0.28) and therefore were combined (n = 35) to yield 8.7 ± 5.2 dB.

Linear regression analysis demonstrated $\langle IL \rangle$ to be independent of GA, $d_{\text{abd wall}}$, d_{ov} and d_{total} for both the FB and EB groups and the combined groups:

$\langle IL \rangle = 0.24GA + 6.3$	$p = 0.39$	EB	(11a)
$\langle IL \rangle = 0.14GA + 6.0$	$p + 0.66$	FB	(11b)
$\langle IL \rangle = 0.27GA + 5.7$	$p = 0.19$	Combined	(11c)

$\langle IL \rangle = 1.3 d_{\text{abd wall}} + 6.5$	$p = 0.39$	EB	(12a)
$\langle IL \rangle = -0.12 d_{\text{abd wall}} + 7.4$	$p = 0.96$	FB	(12b)
$\langle IL \rangle = 1.2 d_{\text{abd wall}} + 6.0$	$p = 0.31$	Combined	(12c)
$\langle IL \rangle = 0.37 d_{\text{ov}} = 7.3$	$p = 0.45$	EB	(13a)
$\langle IL \rangle = -0.34 d_{\text{ov}} + 8.6$	$p = 0.74$	FB	(13b)
$\langle IL \rangle = 0.40 d_{\text{ov}} + 6.6$	$p = 0.31$	Combined	(13c)
$\langle IL \rangle = 0.11 d_{\text{total}} + 8.5$	$p = 0.87$	EB	(14a)
$\langle IL \rangle = -1.2 d_{\text{total}} + 16$	$p = 0.28$	FB	(14b)
$\langle IL \rangle = -0.21 d_{\text{total}} + 10$	$p = 0.71$	Combined	(14c)

The greatest adj r^2 value for these regressions was 0.04 indicating that only 4% of the total variance in $\langle IL \rangle$ is explained by that relationship.

Multiple regression analysis of $\langle IL \rangle$ as a function of the five tissue thicknesses yielded

$$\langle IL \rangle = 14 + 1.3\, d_{\text{abd wall}} - 1.2\, d_{\text{bladder}} - 1.7\, d_{\text{uterus}} - 1.8\, d_{\text{am fluid}} - 0.69\, d_{\text{fetal parts}} \quad (15)$$

where the p values for the six coefficient terms were, respectively, 0.035, 0.35, 0.13, 0.13, <0.13 and 0.41, and for the model, $p = 0.31$.

Tissue models

Two-tailed unpaired t tests between EB and FB groups for $\langle A_{\text{fp}} \rangle_g$, $\langle A_{\text{ho}} \rangle_g$ and $\langle A_{\text{ov}} \rangle_g$ were not considered significant ($p = 0.28$, $p = 0.18$ and $p = 0.96$, respectively) and therefore the two groups for each of these quantities were combined (see Table 2).

Fixed-path tissue model The mean values ± standard deviations and ranges for the *fixed-path* tissue model attenuation coefficients (A_{fp}) for the EB, FB and combined groups are listed in Table 2. Linear regression analysis demonstrated the *fixed-path* tissue model attenuation coefficients to be independent of GA, $d_{\text{abd wall}}$, d_{ov} and d_{total} for both the FB and EB groups and the combined groups:

The greatest adj r^2 value for these regressions was 0.04 indicating that only 4% of the total variance in A_{fp} is explained by that relationship. Figure 4 shows regression eqn (19c) along with the ±90% confidence interval.

Multiple regression analysis of A_{fp} as a function of the five tissue thicknesses yielded

$$A_{\text{fp}} = 5.6 + 0.53\, d_{\text{abd wall}} - 0.51\, d_{\text{bladder}} - 0.71\, d_{\text{uterus}} - 0.73\, d_{\text{am fluid}} - 0.29\, d_{\text{fetal parts}} \quad (20)$$

where the p values for the six coefficient terms were, respectively, 0.0083, 0.35, 0.13, 0.13, 0.13 and 0.41, and for the model, $p = 0.31$.

Homogeneous tissue model. The mean values ± standard deviations and ranges for the *homogeneous* tissue model attenuation coefficients (A_{ho}) for the EB, FB and combined groups are listed in Table 2. Linear regression analysis demonstrated the *homogeneous* tissue model attenuation coefficients to be independent of GA, $d_{\text{abd wall}}$, d_{ov} and d_{total} for both the FB and EB groups and the groups combined (save for one exception):

$A_{\text{fp}} = 0.10 GA + 2.6$	$p = 0.39$	EB	(16a)
$A_{\text{fp}} = 0.059 GA + 2.5$	$p = 0.66$	FB	(16b)
$A_{\text{fp}} = 0.11 GA + 2.4$	$p = 0.19$	Combined	(16c)
$A_{\text{fp}} = 0.53 d_{\text{abd wall}} + 2.7$	$p = 0.39$	EB	(17a)
$A_{\text{fp}} = -0.048 d_{\text{abd wall}} + 3.1$	$p = 0.96$	EB	(17b)
$A_{\text{fp}} = 0.52 d_{\text{abd wall}} + 2.5$	$p = 0.31$	Combined	(17c)
$A_{\text{fp}} = 0.15 d_{\text{ov}} + 3.0$	$p = 0.45$	EB	(18a)
$A_{\text{fp}} = -0.22 d_{\text{ov}} + 1.7$	$p = 0.10$	FB	(18b)
$A_{\text{fp}} = 0.17 d_{\text{ov}} + 2.8$	$p = 0.31$	Combined	(18c)
$A_{\text{fp}} = 0.045 d_{\text{total}} + 3.6$	$p = 0.87$	EB	(19a)
$A_{\text{fp}} = -0.49 d_{\text{total}} + 6.9$	$p = 0.28$	FB	(19b)
$A_{\text{fp}} = -0.086 d_{\text{total}} + 4.3$	$p = 0.71$	Combined	(19c)

$A_{ho} = 0.0044GA + 0.51$	$p = 0.81$	EB	(21a)
$A_{ho} = -0.0017GA + 0.41$	$p = 0.93$	FB	(21b)
$A_{ho} = 0.0091GA + 0.41$	$p = 0.49$	Combined	(21c)
$A_{ho} = -0.034d_{abd\ wall} + 0.64$	$p = 0.71$	EB	(22a)
$A_{ho} = -0.067d_{abd\ wall} + 0.53$	$p = 0.67$	FB	(22b)
$A_{ho} = -0.022d_{abd\ wall} + 0.56$	$p = 0.78$	Combined	(22c)
$A_{ho} = -0.017d_{ov} + 0.66$	$p = 0.58$	EB	(23a)
$A_{ho} = -0.051d_{ov} + 0.60$	$p = 0.42$	FB	(23b)
$A_{ho} = -0.0077d_{ov} + 0.56$	$p = 0.76$	Combined	(23c)
$A_{ho} = -0.062d_{total} + 1.0$	$p = 0.14$	EB	(24a)
$A_{ho} = -0.11d_{total} + 1.3$	$p = 0.083$	FB	(24b)
$A_{ho} = -0.076d_{total} + 1.1$	$p = 0.026$	Combined	(24c)

The greatest adj r^2 value for these regressions was 0.24 indicating that only 24% of the total variance in A_{ho} is explained by that relationship. Figure 5 shows regression eqn (24c) along with the ±90% confidence interval.

Multiple regression analysis of A_{ho} as a function of the five tissue thicknesses yielded

$$A_{ho} = 1.3 + 0.0091\ d_{abd\ wall} - 0.13\ d_{bladder} - 0.17\ d_{uterus} - 0.17\ d_{am\ fluid} - 0.11\ d_{fetal\ parts} \quad (25)$$

where the p values for the six coefficient terms were, respectively, 0.0001, 0.91, 0.10, 0.19, 0.17 and 0.41, and for the model, $p = 0.077$.

Overlying tissue model. The mean values ± standard deviations and ranges for the *overlying* tissue model attenuation coefficients (A_{ov}) for the EB, FB and combined groups are listed in Table 2. Linear regression analysis demonstrated the *overlying* tissue model attenuation coefficients to be independent of *GA* and $d_{abd\ wall}$ for both the FB and EB groups and the groups combined, and dependent on d_{ov} and d_{total} for the EB and combined group:

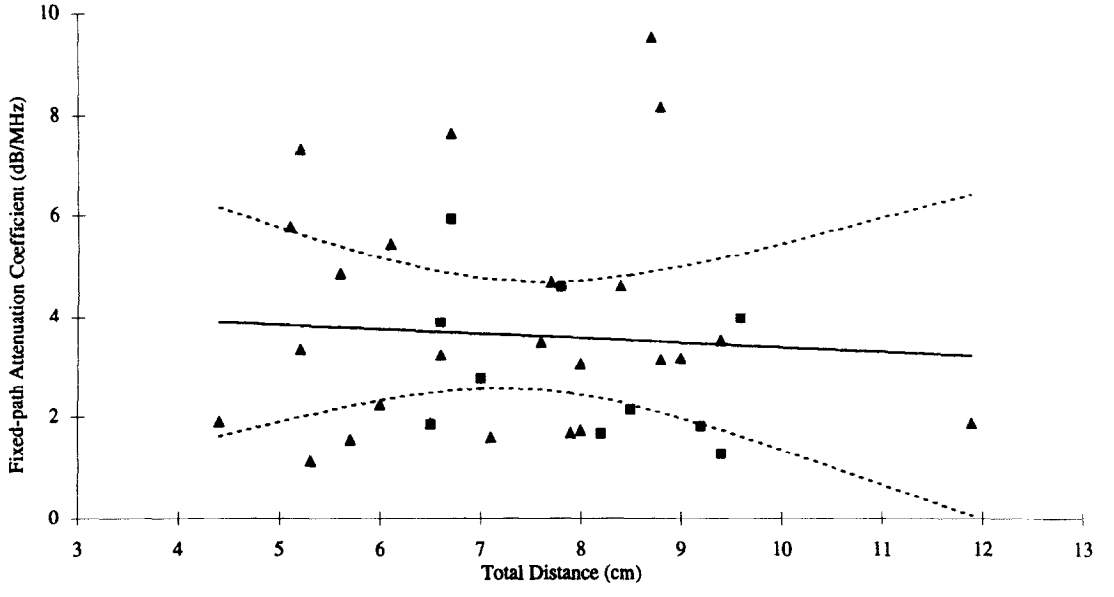

Fig. 4. Regression (solid line: see eqn 19c) and ±90% confidence intervals (dashed lines) of the *fixed-path* attenuation coefficient as a function of total distance for the combined data set (EB: ▲ and FB: ●).

$A_{ov} = -0.040GA + 1.3$	$p = 0.20$	EB	(26a)
$A_{ov} = -0.031GA + 1.1$	$p = 0.52$	FB	(26b)
$A_{ov} = -0.030GA + 1.2$	$p = 0.16$	Combined	(26c)
$A_{ov} = -0.20d_{abd\ wall} + 1.3$	$p = 0.15$	EB	(27a)
$A_{ov} = -0.30d_{abd\ wall} + 1.4$	$p = 0.41$	FB	(27b)
$A_{ov} = -0.21d_{abd\ wall} + 1.3$	$p = 0.093$	Combined	(27c)
$A_{ov} = -0.13d_{ov} + 1.5$	$p = 0.003$	EB	(28a)
$A_{ov} = -0.22d_{ov} + 1.7$	$p = 0.10$	FB	(28b)
$A_{ov} = -0.13d_{ov} + 1.5$	$p = 0.0012$	Combined	(28c)
$A_{ov} = -0.15d_{total} + 1.9$	$p = 0.020$	EB	(29a)
$A_{ov} = -0.27d_{total} + 3.0$	$p = 0.069$	FB	(29b)
$A_{ov} = -0.16d_{total} + 2.0$	$p = 0.0043$	Combined	(29c)

The greatest adj r^2 value for these regressions was 0.28 indicating that only 28% of the total variance in A_{ov} is explained by that relationship. Figure 6 shows regression eqn (29c) along with the ±90% confidence interval.

Multiple regression analysis of A_{ov} as a function of the five tissue thicknesses yielded

$$A_{ov} = 1.8 - 0.044\ d_{abd\ wall} - 0.12\ d_{bladder} - 0.25\ d_{uterus} - 0.058\ d_{am\ fluid} - 0.18\ d_{fetal\ parts} \quad (30)$$

where the p values for the six coefficient terms were, respectively, 0.0003, 0.72, 0.11, 0.17, 0.57 and 0.21, and for the model, $p = 0.012$.

DISCUSSION

We have previously reported that *in vivo* ultrasound exposure of the human ovary during a diagnostic ultrasound examination of 43 nonpregnant women is an order of magnitude less than the maximum values of ultrasonic quantities measured *in vitro* (Siddiqi et al. 1991). Our current studies confirm this hypothesis to be also true in the case of routine "diagnostic" obstetric ultrasound examination of the human embryo and fetus wherein the $\langle IL \rangle_g$ is 8.5 ± 2.2 dB and 11 ± 6.0 dB for first- and second-trimester empty bladder conditions, respectively (see Table 1). Additionally, despite the significant difference ($p = 0.02$) in gestational age between the EB and FB groups (12 ± 4.1

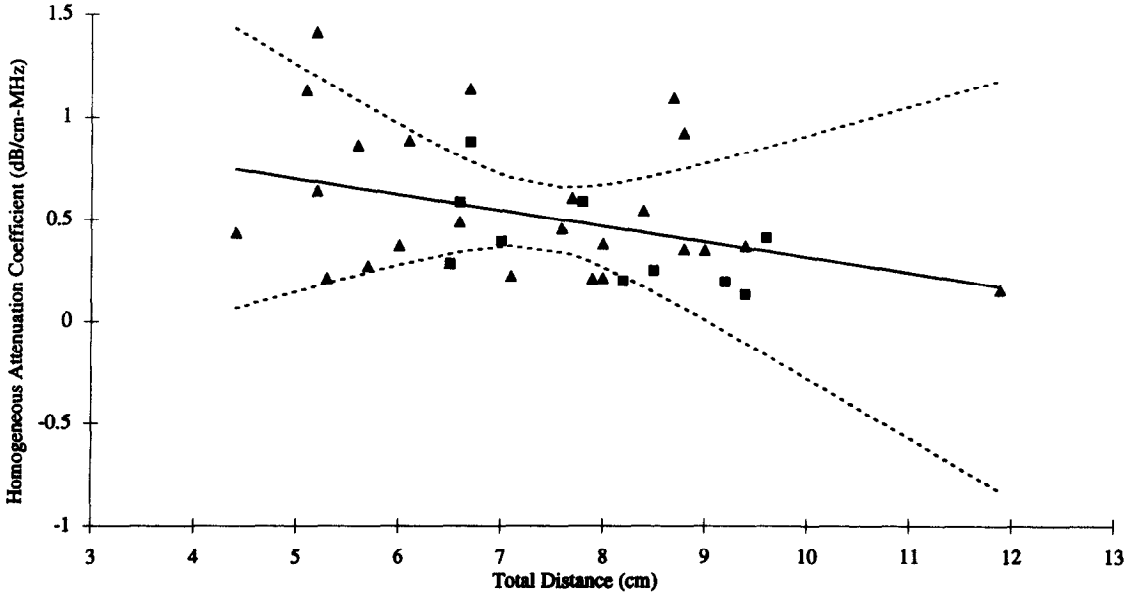

Fig. 5. Regression (solid line: see eqn 24c) and ±90% confidence intervals (dashed lines) of the *homogeneous* attenuation coefficient as a function of total distance for the combined data set (EB: ▲ and FB: ●).

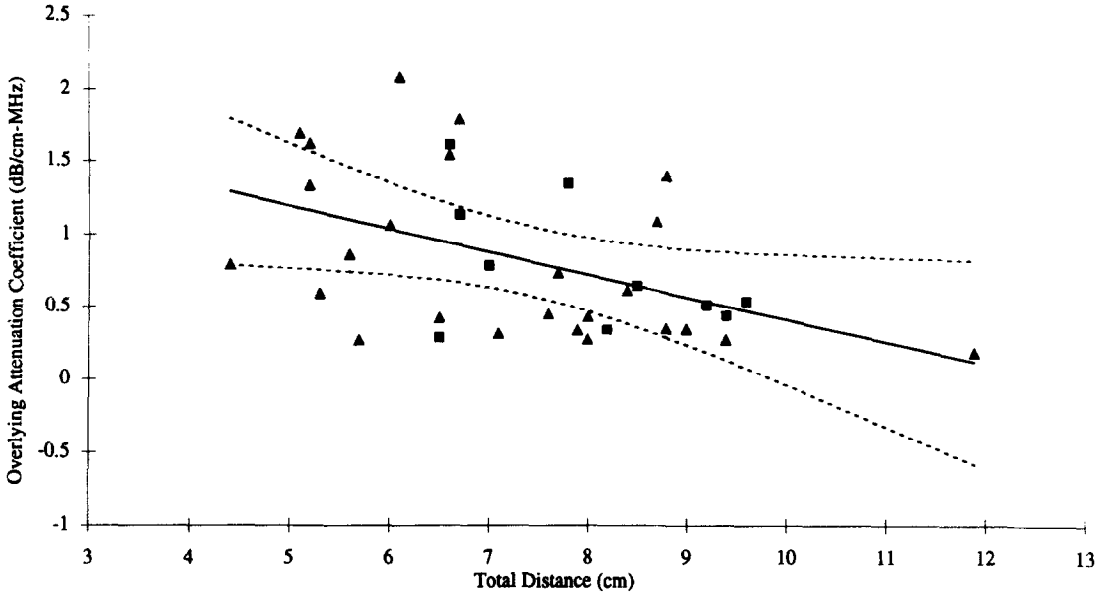

Fig. 6. Regression (solid line: see eqn 29c) and ±90% confidence intervals (dashed lines) of the *overlying* attenuation coefficient as a function of total distance for the combined data set (EB: ▲ and FB: ●).

weeks and 8.6 ± 4.1 weeks, respectively—see Table 2), there was no statistically significant difference in the $\langle IL \rangle_g$ between EB and FB groups ($p = 0.28$), that is, 9.3 ± 5.6 dB and 7.2 ± 3.7 dB, respectively (see Table 2). We also estimated (Siddiqi et al. 1991) the *fixed-path* and *overlying* attenuation coefficients from the 43 nonpregnant women to be $\langle A_{fp} \rangle_g = 3.0 \pm 1.7$ dB/MHz and $\langle A_{ov} \rangle_g = 0.72 \pm 0.62$ dB/cm-MHz. These estimates compare favorably with those estimated in this study ($\langle A_{fp} \rangle_g = 3.6 \pm 2.2$ dB/MHz and $\langle A_{ov} \rangle_g = 0.82 \pm 0.54$ dB/cm-MHz).

In our current study, $\langle IL \rangle_g$ for both the EB and FB groups individually or combined was independent of GA, $d_{abd\ wall}$, d_{ov} and d_{total} (see eqns 11–14). We previously estimated (Siddiqi et al. 1992) the *in situ* attenuation coefficients of both the anterior abdominal wall ($A_{abd\ wall} = 1.4$ dB/cm-MHz) and the uterus ($A_{uterus} = 0.14$ dB/cm-MHz) from *in vivo* exposimetry measurements from 23 nonpregnant women (nulliparas = 14, multiparas = 9) under both full bladder and empty bladder conditions. These results suggested that the abdominal wall is the principal source of ultrasonic energy loss in a reproductive, transabdominal ultrasound examination where multiple regression analysis provided the best fit ($p = 0.056$), *i.e.*, $IL_{abd\ wall} = 2.8\ (d_{abd\ wall})^{0.99}$. Based on these data and the assumption that the thickness of the anterior abdominal wall does not change significantly during the first 20 weeks of gestation (see Tables 1 and 2), the $\langle IL \rangle$ would be expected to be independent of GA and d_{total} for either the EB or FB groups individually or when combined (see eqns 11 and 15). The absence of any significant correlation between $\langle IL \rangle$ and $d_{abd\ wall}$ and d_{ov} is more difficult to explain. We suggest that beginning in the second trimester and extending into the early third trimester, there are changes in body fat and water content during normal human pregnancy (Pipe et al. 1979). The greatest gain in fat is over the abdomen where the skin thickness increases by about 40% (Hytten 1980). Similarly, for women without clinically evident edema, the extracellular water content expands by approximately 1 to 2 L (Hytten et al. 1966). These physiologic changes may partially explain the absence of any significant correlation between $\langle IL \rangle$ and $d_{abd\ wall}$ and d_{ov}.

All distance measurements from the sonogram image were made from an imaging system that assumes a propagation speed of 1540 m/s which could pose an error in actual distances for which the propagation speed is different from that of 1540 m/s. However, this does not create an uncertainty in the distance measurements or, for that matter, in the calculation of the various attenuation coefficients. A worst case uncertainty of tissue propagation speeds of 1540 ± 40 m/s (a ±2.6% uncertainty) yields a ±2.6% uncertainty in the distance determination. This is much less than the standard deviations of distance (see Table 1) which range from 20% of the mean value.

Despite our above assertion, using our previously acquired data (Siddiqi et al. 1992) ($A_{abd\ wall} = 1.4$ dB/cm-MHz and $A_{uterus} = 0.14$ dB/cm-MHz), we developed an insertion loss prediction equation based on the sum of the insertion losses from the anterior abdominal wall and uterus (assuming all fluid paths to be lossless):

$$\langle IL\rangle_{\text{predicted}} = A_{\text{abd wall}} d_{\text{abd wall}} f_c + A_{\text{uterus}} d_{\text{uterus}} f_c \quad (31)$$

$$= 1.4\, d_{\text{abd wall}} f_c + 0.14\, d_{\text{uterus}} f_c \quad (32)$$

where f_c is the center frequency. Equation 32 was then used to predict the insertion loss for each of the 35 examinations reported herein and was then compared to the measured insertion loss, $\langle IL\rangle_{\text{measured}}$.

In Table 3 are shown the insertion loss estimated from the measurements reported herein ($\langle IL\rangle_{\text{measured}} = \langle IL\rangle_g$ from Table 2) and the predicted insertion loss ($\langle IL\rangle_{\text{predicted}}$) as well as the insertion loss error (IL_{error}), defined as

$$IL_{\text{error}} = \left(\frac{\langle IL\rangle_{\text{predicted}} - \langle IL\rangle_{\text{measured}}}{\frac{1}{2}(\langle IL\rangle_{\text{predicted}} + \langle IL\rangle_{\text{measured}})} \right) \times 100. \quad (33)$$

Two-tailed unpaired t tests between EB and FB groups for $\langle IL\rangle_{\text{measured}}$, $\langle IL\rangle_{\text{predicted}}$ and IL_{error} were not considered significant ($p = 0.28$, $p = 0.46$ and $p = 0.57$, respectively) and therefore the two groups for each of these quantities were combined. The mean value of IL_{error} was independent of GA ($p = 0.28$) and d_{total} ($p = 0.48$). While the mean value of IL_{error} (see Table 3) for the combined groups was 0.39%, a two-tailed, paired t test between $\langle IL\rangle_{\text{measured}}$ and $\langle IL\rangle_{\text{predicted}}$ was not considered significant ($p = 0.33$).

When we attempted to predict $\langle IL\rangle$ from our earlier work, the IL_{error} as listed in Table 3 did not appear too great considering the complexity of the entire measurement procedure and the physiologic changes known to occur in body fat and water content during normal pregnancy. We therefore believe that predicting the insertion loss from our earlier work appears quite reasonable and does not call into question either this or the earlier study. In fact, we are heartened to note that this approach to predicting the *in utero* intensity during a routine obstetric ultrasound examination is feasible.

Table 3. Mean value ± standard deviation of calculated quantities of $[IL)_{\text{measured}}$ is the insertion loss estimated from the measurements reported herein, $\langle IL\rangle_{\text{predicted}}$ is the predicted insertion loss (see eqn 32) and IL_{errors} is the insertion loss error (see eqn 33).

	EB group (n = 25)	FB group (n = 10)	EB versus FB p value†	Groups combined (n = 35)
$\langle IL\rangle_{\text{measured}}$ (dB)	9.3 ± 5.6	7.2 ± 3.7	0.28	8.7 ± 5.2
$\langle IL\rangle_{\text{predicted}}$ (dB)	8.0 ± 2.8	7.3 ± 1.9	0.46	7.8 ± 2.5
IL_{error} (%)	−3.2 ± 60	9.4 ± 55	0.57	0.39 ± 58

† Unpaired Student t test.

The *fixed-path* (A_{fp}), *homogeneous* (A_{ho}) and *overlying* (A_{ov}) attenuation coefficients for their respective tissue models all appear to be independent of bladder state, GA and $d_{\text{abd wall}}$.

The *fixed-path* attenuation coefficient is also independent of d_{ov} and d_{total}. This suggests that $\langle A_{\text{fp}}\rangle_g$ of 3.6 ± 2.2 dB/MHz could be applied independent of input about bladder state, GA, $d_{\text{abd wall}}$, or d_{ov}, and specifically d_{total} as shown in the regression (see Fig. 4). Should the most conservative approach be desired ("maximum" exposure), then an $\langle A_{\text{fp}}\rangle_g$ value of 1.1 dB/MHz (the minimum value for all cases considered) could be applied (note that one standard deviation from the mean is 1.5 dB/MHz) which is a factor of 3.2 less than the mean value. This approach obviously assumes that our sample size is truly representative of the population exposed to ultrasound and the value 1.1 dB/MHz is a true absolute minimum. The NRCP (1992) has recommended the use of the *fixed-path* attenuation coefficient values of 1.0 and 0.75 dB/MHz for first- and second-trimester obstetrical applications, respectively. These values are based on a worst-case ("maximum" exposure) approach and are consistent with the results of our study since no value was less than 1.0 dB/MHz, but inconsistent because there is no evidence that A_{fp} varies with gestational age up to about 20 weeks.

Both A_{ho} and A_{ov} are however dependent on d_{total} for the combined groups (see eqns 24c and 29c and Figs. 5 and 6). The *homogeneous* attenuation coefficient ($\langle A_{\text{ho}}\rangle_g$) for the combined groups is 0.52 ± 0.33 dB/cm-MHz. One standard deviation from the mean is 0.19 dB/cm-MHz and the minimum value of A_{ho} is 0.14 dB/cm-MHz (in the FB group). For all applications of diagnostic ultrasound, FDA's Center for Devices and Radiological Health uses for regulatory purposes a derating factor, based on the *homogeneous* tissue model, of 0.3 dB/cm-MHz (FDA 1985, 1993) and the Output Display Standard (AIUM/NEMA 1992) has recommended this same value. The mean and one standard deviation values of the results reported herein compare favorably with this value of 0.3 dB/cm-MHz (see Fig. 5). Applying the *homogeneous* tissue model for estimating the "maximum" exposure in terms of predicting the highest *in utero* intensity from these results would require use of the value 0.14 dB/cm-MHz which is a factor of 3.7 less than the mean value.

The *overlying* attenuation coefficient ($\langle A_{\text{ov}}\rangle_g$) for the combined groups is 0.82 ± 0.62 dB/cm-MHz. One standard deviation from the mean is 0.10 dB/cm-MHz and the minimum value of A_{ov} is 0.19 dB/cm-MHz

(in the FB group). Thus, applying the *overlying* tissue model, the "maximum" exposure in terms of predicting the highest *in utero* intensity from these results is, therefore, 0.19 dB/cm-MHz which is a factor of 4.3 less than the mean value.

In summary, any one of the three tissue models may be used to estimate *in utero* acoustic quantities during the first and second trimesters of human pregnancy based on this study. All three tissue models yield a mean value of about a factor of 3 to 4 greater than their respective minimum values. We have provided the lowest values for these attenuation coefficients from our *in vivo* studies so that "maximum" exposure intensity estimates are also feasible for any given exposure condition. In the case of the *overlying* and *homogeneous* tissue models, there was a statistically significant correlation between their calculated attenuation coefficients and d_{total} for the combined data set whereas there was no such dependency for the calculated *fixed-path* tissue model. We speculate that as we collect more data, either the *homogeneous* or the *overlying* tissue models will prove to be the best model for estimating *in utero* ultrasound intensity during routine obstetrical sonography.

Acknowledgements—Supported in part by NIH Grants HD21687, HD20748 and CA09067.

REFERENCES

Akaiwa, A. Ultrasonic attenuation character estimated from backscattered radio frequency signals in obstetrics and gynecology. Yonago Acta Medica 32:1–10; 1989.

American Institute of Ultrasound in Medicine. Bioeffects consideration for the safety of diagnostic ultrasound. J. Ultrasound Med. 7 (Suppl):S1–S38; 1988.

American Institute of Ultrasound in Medicine. Acoustic output measurement and labeling standard for diagnostic ultrasound equipment. Rockville, MD: AIUM Publications; 1992.

American Institute of Ultrasound in Medicine/National Electrical Manufacturers Association. Standard for real-time display of thermal and mechanical acoustic output indices on diagnostic ultrasound equipment. Rockville, MD: AIUM Publications; 1992.

American Institute of Ultrasound in Medicine. Bioeffects and safety of diagnostic ultrasound. Rockville, MD: AIUM Publications; 1993.

Carson, P. L.; Rubin, J. M.; Chiang, E. H. Fetal depth and ultrasound path lengths through overlying tissues. Ultrasound Med. Biol. 15:629–639; 1989.

Carson, P. L. Constant soft tissue distance model in pregnancy. Ultrasound Med. Biol. 15:27–29; 1989.

Daft, C. M. W.; Siddiqi, T. A.; Fitting, D. W.; Meyer, R. A.; O'Brien, W. D., Jr. *In vivo* fetal ultrasound exposimetry. IEEE Trans. Ultrason. Ferroelect. Freq. Contr. 37:501–505; 1990.

Food and Drug Administration. Guide for measuring and reporting acoustic output of diagnostic ultrasound medical devices. Document 510(k). Rockville, MD: US Department of Health and Human Services, FDA, Center for Devices and Radiological Health; 1985.

Food and Drug Administration. Revised 510(k) diagnostic ultrasound guidance for 1993. Rockville, MD: US Department of Health and Human Services, FDA, Center for Devices and Radiological Health; February 17, 1993.

Hamburg, M. Basic statistics: A modern approach, 2nd ed. New York: Harcourt Brace Jovanovich, Inc.; 1979:272–273.

Hytten, F. E.; Thomas, A. M.; Taggart, N. Total body water in normal pregnancy. J. Obstet. Gynaecol. Brit. Commonw. 73:553–561; 1966.

Hytten, F. E. Weight gain in pregnancy. In: Hytten, F. E.; Chamberlain, G., eds. Clinical physiology in obstetrics, 1st ed. Oxford: Blackwell Scientific Publications; 1980:223–227.

Miller, M. W.; Ziskin, M. C. Biological consequences of hyperthermia. Ultrasound Med. Biol. 15:707–722; 1989.

National Council on Radiation Protection and Measurements. Biological effects of ultrasound: Methods and clinical implications. NCRP Report No. 74. Bethesda, MD; 1983.

National Council on Radiation Protection and Measurements. Exposure criteria for medical diagnostic ultrasound: I. Criteria based on thermal mechanisms. NCRP Report No. 113. Bethesda, MD; 1992.

National Institutes of Health. The use of diagnostic ultrasound imaging in pregnancy. National Institute of Child Health and Development Conference process. Washington, D.C.: U.S. Government Printing Office; 1984.

O'Brien, W. D., Jr. Ultrasound bioeffects related to obstetrical sonography. In: Fleischer, A. C.; Jeanty, P.; Manning, F.; Romero, R. E., eds. The principles and practice of ultrasonography in obstetrics and gynecology, 4th ed. Norwalk, CT: Appleton and Lange; 1991:15–23.

O'Brien, W. D., Jr. Ultrasound dosimetry and interaction mechanisms. In: Greene, M. W., ed. Non-ionizing radiation: Proceedings of the second international non-ionizing radiation workshop. Vancouver, BC: Canadian Radiation Protection Association; 1992:151–172.

Pipe, N. G. J.; Smith, T.; Halliday, D.; Edmonds, C. J.; Williams, C.; Coltart, T. M. Changes in fat, fat-free mass and body water in human normal pregnancy. Br. J. Obstet. Gynaecol. 86:929–940; 1979.

Ramnarine, K. V.; Nassiri, D. K.; Pearce, J. M.; Joseph, A. E. A.; Patel, R. H.; Varma, T. R. Estimation of *in situ* ultrasound exposure during obstetric examinations. Ultrasound Med. Biol. 19:319–329; 1993.

Siddiqi, T. A.; O'Brien, W. D., Jr.; Meyer, R. A.; Sullivan, J. M.; Miodovnik, M. *In situ* exposimetry: The ovarian ultrasound examination. Ultrasound Med. Biol. 17:257–263; 1991.

Siddiqi, T. A.; O'Brien, W. D., Jr.; Meyer, R. A.; Sullivan, J. M.; Miodovnik, M. Human *in situ* dosimetry: Differential insertion loss during passage through abdominal wall and myometrium. Ultrasound Med. Biol. 18:681–689; 1992.

Smith, S. W.; Stewart, H. F.; Jenkins, D. P. A plane layered model to estimate *in situ* ultrasound exposures. Ultrasonics 23:31–40; 1985.

Tarantal, A. F.; O'Brien, W. D., Jr. Discussion of ultrasonic safety related to obstetrics. In: Sabbagha, R. E., ed. Diagnostic ultrasound applied to obstetrics and gynecology, 3rd ed. Philadelphia, PA: J. B. Lippincott Company; 1994:45–56.

World Federation for Ultrasound in Medicine and Biology. Second WFUMB Symposium on Safety and Standardization in Medical Ultrasound. Kossoff, G.; Nyborg, W. L., eds. Ultrasound Med. Biol. 15 (Suppl. 1):1–116; 1989.

World Federation for Ultrasound in Medicine and Biology. WFUMB Symposium on Safety and Standardization in Medical Ultrasound: Issues and Recommendations Regarding Thermal Mechanisms for Biological Effects of Ultrasound. Barnett, S. B.; Kossoff, G., eds. Ultrasound Med. Biol. 18:731–814; 1992.

Ziskin, M. C.; Pittiti, D. B. Epidemiology of human exposure to ultrasound: A critical review. Ultrasound Med. Biol. 14:91–96 1988.